# SpaCal detector calibration for 2004 data analyses

Ryszard Maculewicz
Adam Mickiewicz University, Poznan
Faculty of Physics
Email: maculewicz@dr.com

*The H1 group, that I worked at performs fundamental research in the field of High Energy Physics. The main topic of my work was a SpaCal detector calibration for 2004 data analysis. For the data analysis I used H100 environment 2.6.4 version. All results were prepared as ROOT plots. The report contains a short introduction to H1 experiment, description of H1 detector and finally a SpaCal calibration including the results of my work.*

## 1 Introduction

### *1.1 HERA and H1*

HERA (Hadron-Electron Ring-Angle) is a facility where electrons and protons are accelerated to high collision energies in two storage rings one for protons of 920 GeV, and one for electrons (positrons) of $\sim$ 30 GeV. In an underground tunnel in Hamburg, two beams circulate in opposite directions and in two interaction points there is the collision between protons and electrons. Products of the collision are measured by the e.g. H1 detector.

The H1 detector was built, and is operated by the H1 group. The main field of their research is to measure the structure of the proton, the study the fundamental interactions between particles, and the search the physics beyond the Standard Model of elementary particles. [1]

The detector was designed in such a way that is able to detect and measure energetic particles and jets, which are emitted as a result of collisions between electrons and protons. Special emphasis was placed on the identification of these particles, especially electrons and muons. The fact that protons enter into the interaction zone with a much higher energy than electrons was also very important during the designing.

```
The H1 detector consists of:

1. Beam pipe and beam magnets
2. Central tracking chambers
3. Forward tracking and transition radiators
4. Electromagnetic Calorimeter (lead, liquidargon)
5. Hadronic Calorimeter (stainess steel)
6. Superconducting coil (1,2T)
7. Compensating magnet
8. Helium cryogenics
9. Muon cambers
10. Return yoke (instrumented iron with streamer tubes)
11. Muon-Toroid-Magnet
12. Warm calorimeter (SpaCal)
13. (Does not exist anymore)
14. Concrete screen
15. Liquid Argon cryostat
```

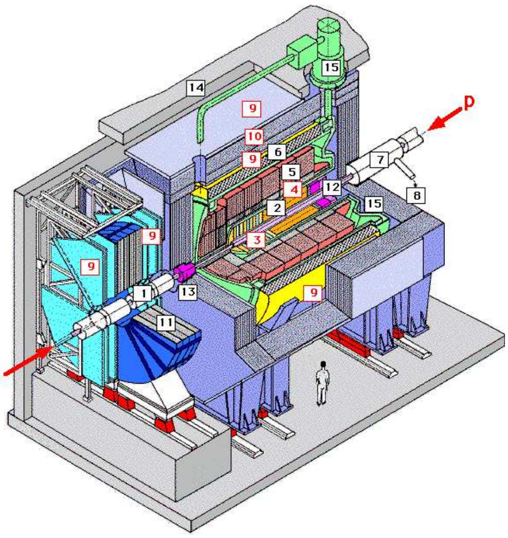

Fig. 1: *The H1 detector.*

## *1.2 SpaCal Calorimeter*

The SpaCal calorimeter comprises the electromagnetic and hadronic sections. The electromagnetic part of the SpaCal consists of 1192 cells with an active volume of $4.05 \times 4.05 \times 25\text{cm}^3$ each. The cells are made of grooved lead plates and scintillating fibers with a diameter of 0.5 mm.

The scintillation light from each cell is converted into an electric pulse using photomultiplier tubes (PMT). The active length of the electromagnetic SpaCal corresponds to 27.47 radiation lengths and 1 hadronic interaction length. The angular coverage of the calorimeter is $135^o < \Theta < 177.8^o$.

The hadronic part of the SpaCal comprises 136 cells of $12 \times 12 \times 25$ cm$^3$ providing one nuclear interaction length. The fibers are of the same type as in the electromagnetic section but have a larger diameter of 1mm. The hadronic resolution of the calorimeter is about $\frac{30\%}{\sqrt{E}}$[2]

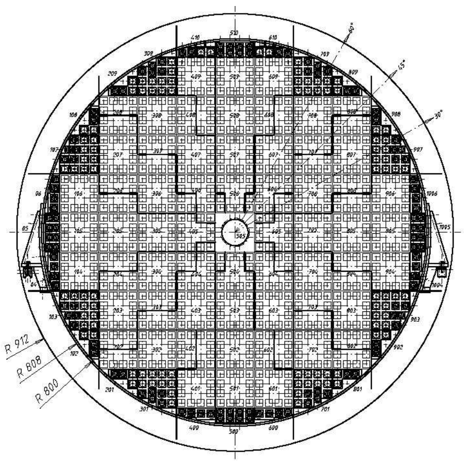

Fig. 2: *Transverse view of the SpaCal. Small boxes indicate individual cells.They are combinated in 4x4 groups into super modules.*

## 2 SpaCal calibration

The energy measured in the SpaCal calorimeter is the energy coming from each cell of the calorimeter and it is done by using a photomultiplier tube for each cell. Therefore, all amplification gains have to be known to define the SpaCal energy scale. A special LED calibration system was developed in order to detect these variations. The LED information is written to the database and used for the SpaCal energy reconstruction. The offline analysis showed that the result of SpaCal energy is stable in time up to about 1 % precision. The offline SpaCal cell-dependent calibration for 1996 data was preformed using the kinematic peak for $R_{spacal} < 50$ cm and cosmic muons for the outher region. Time-dependent factors were applied. The double angle method was applied additionally to this calibration.

### *2.1 SpaCal energy calibration*

The calibration of the SpaCal energy response is done by the LED system, which feeds light through fibers into light mixers PMTs. Potential time-dependent instabilities of the light output of each LED are monitored by photodiodes. The Calorimeter was calibrated using the so called "kinematic peak" calibration method.

The double angle calibration method, which is used in this work makes use of the fact that the event kinematics is over overconstrained. This leads to the possibility to determine the scattering electron energy, $E_{DA}$, via the measurement of its polar angle, $\Theta_e$, and of the hadronic final state polar angle, $\Theta_h$,

$$E_{DA} = \frac{E_e(1 - y_{DA})}{\sin^2(\Theta_e/2)} \tag{1}$$

Where

$$y_{DA} = \frac{\tan(\Theta_h/2)}{\tan(\Theta_h/2) + \tan(\Theta_e/2)} \tag{2}$$

As it can be seen from the relations, the double angle method does not depend directly on the SpaCal. The resolution of the double angle reconstruction method is about three times better than of the SpaCal, and that is why it was used to define the reference energy scale for the SpaCal calibration.

#### 2.1.1 Cell-by-cell correction

For each cell belonging to a particular cluster the pull/delta of the whole cluster is plotted in a histogram, weighted by the energy fraction contribution of the cell to the cluster.

$$E_{sp} = \sum_i E_i \cdot \delta^i \tag{3}$$

Where $E_i$ is the energy of the cluster cell. In order to separate the influence of single cells in a cluster we need a number of iteration. In every step of the iteration the result from the previous iteration is used and further correction to cell energies is calculated. About five interactions are sufficient to obtain a stable result.[3]

The SpaCal calibration task can be expressed as a minimization of the following function:

$$S(\Delta g_{ic}) = \sum_{ev}(E^{ev}_{calibr} - \sum_{ic} E^{ev}_{calibr}(1 + \Delta g_{ic}))^2 \rightarrow \min. \tag{4}$$

The first summation is performed over all selected events while the second one extends over all cells included in the electrons cluster. $E^{ev}_{calibr}$ defines the energy scale of the event to which the calibration is performed, in our case it is equal to $E^{ev}_{DA} \cdot E^{ev}_{ic}$ corresponds to the energy measured by the cell (ic) for the event (ev). This energy includes all corrections done before the final calibration. $\Delta g_{ic}$ is the correction to the amplification gain factor of the cell (ic) to be determined.

In the general, the minimisation of the function (4) requires to solve a system of 1192 equations with 1192 variables. In principle, it can be done since many of the non-diagonal elements in the correlation matrix are equal to 0. However, many problems occur during this minimisation which for example, are due to the non-Gausian tails of the energy response.

Instead the following interactive procedure was used here. For each event, the event miscalibration or event pull was introduced:

$$\delta_{ev} = \frac{\sum_{ic} E_{ic}^{ev}(1 + \Delta^{it} g_{ic})}{E_{cluster}^{ev}} = \frac{E_{cluster}^{ev}}{E_{calibr}^{ev}}, \tag{5}$$

here it is denotes the iteration number with $\delta^1 g_{ic} = 0$ for the first iteration. The relative contribution of the cell j to the event pull is given by the fraction of energy deposited in it.:

$$w_j^{ev} = \frac{E_j^{ev}(1 + \Delta^{it} gj)}{E_{cluster}^{ev}} \tag{6}$$

By construction the sum of the weights $w_j^{ev}$ for any event is equal to 1. Finally the weighted pull average over all events with removing of outliers was calculated and the correction of all cell amplification gain factors was obtained:

$$\Delta^{it+1} gj = \Delta^{it} gj - (\overline{\delta_{ev} w^{ev} j} - 1). \tag{7}$$

The iterative procedure was continued until $\{mathrmmax_j(\overline{\delta_{ev} w^{ev} j}) < 0.002$. [2]

#### 2.1.2 Inbox correction

Due to the SpaCal calorimeter construction there are small effects on the reconstructed energy expected from the position of the particle impact point with in the calorimeter cells. In case, when a particle hits a calorimeter cell in the middle, the energy is better contained then in the case of a hiting a cell corner, when part of the energy is lost in the dead material and not detected. To correct this effect the energy pull $\delta$ after cell-by-cell calibration is investigated as a function of the impact point position within the hottest cell in the cluster.

#### 2.1.3 Crack correction

Except for the dead material between single cells, the SpaCal is constructed from larger blocks of 16 cells, so called, supermodules. Hence, there are further energy losses due to cracks between supermodules. There where corrected as a function of $R_{box} = \max(|x_{Sp}|, |y_{Sp}|)$, where the coordinates to the impact point position.

#### 2.1.4 Radial correction

That is the lowest correction introduced in this analysis. It is motivated by the observed fluctuations of the energy pull $\delta$ as a function of the radius in the SpaCal plane $R_{Sp} = \sqrt{(x_{Sp})^2 + (y_{Sp})^2}$. Hereafter the radial corrections are used to correct the reconstructed cluster energy. [3]

## 3 Results of the calibration

The plots below present calibration results in subsequent correction steps.

### *3.1 Ratio before calibration*

The figure below presents the $\frac{E_{DA}}{E_{Spacal}}$ ratio before the cell-by-cell correction.

The plot shows strange behaviour especially in the part, where it goes down. An explanation for this wwould require further study.

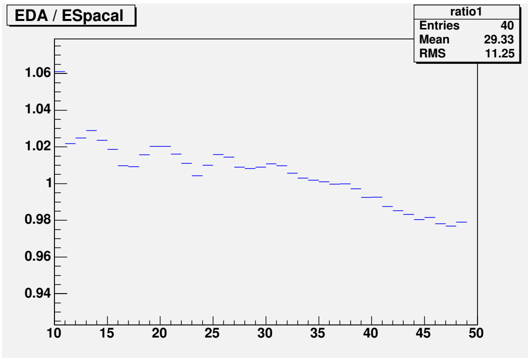


Fig. 3: *Ratio before calibration.*

## 3.2 Ratio after cell-by-cell correction

The figure below present $\frac{E_{DA}}{E_{Spacal}}$ ratio before (blue) and after (red) the cell-by-cell correction.

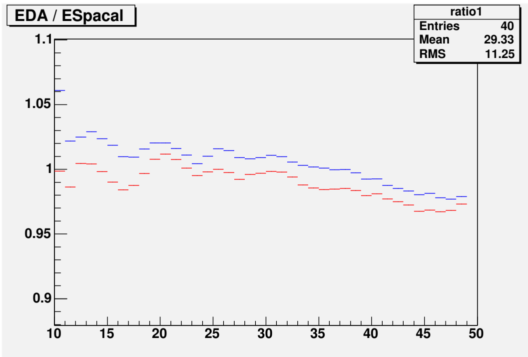


Fig. 4: *Ratio after cell-by-cell correction.*

## 3.3 Ratio after inbox correction

The figure below presents the $\frac{E_{DA}}{E_{Spacal}}$ ratio before (red) and after (green) the inbox correction.

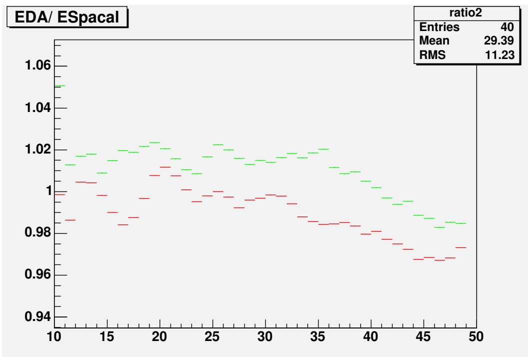


Fig. 5: *Ratio after inbox correction.*

## 3.4 Ratio after crack correction

The figure below presents the $\frac{E_{DA}}{E_{Spacal}}$ ratio before (green) and after (black) the crack correction.

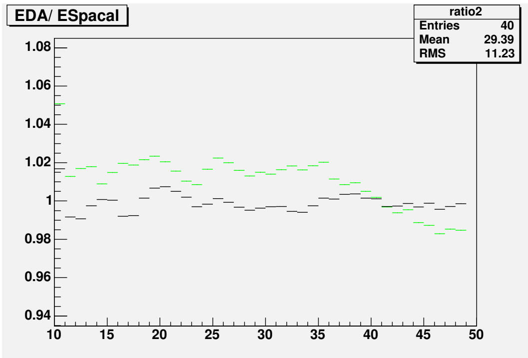


Fig. 6: *Ratio after crack correction.*

## 3.5 *Ratio after radial correction*

The figures below presents the $\frac{E_{DA}}{E_{Spacal}}$ ratio before (black) and after (continous) the radial correction and enlarged $\frac{E_{DA}}{E_{Spacal}}$ ratio after the radial correction.

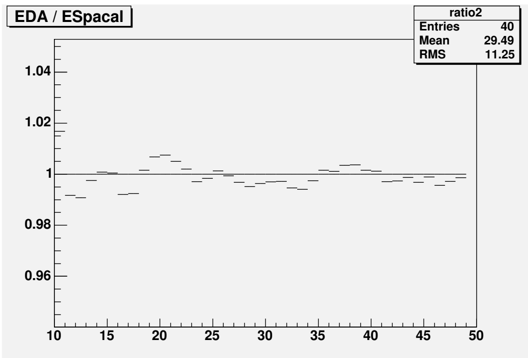


Fig. 7: *Ratio after radial correction.*

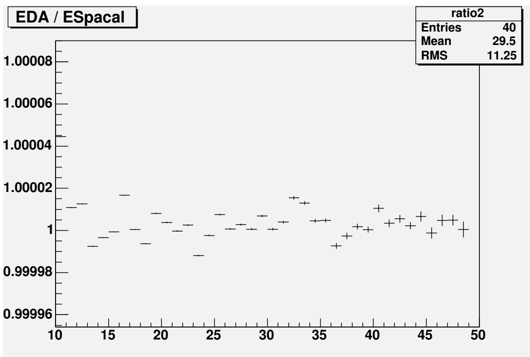


Fig. 8: *Ratio after radial correction.*

## 3.6 *Kinematic peak*

The figure below presents the kinematic peak. It shows the difference between the electron energy before and after calibration.

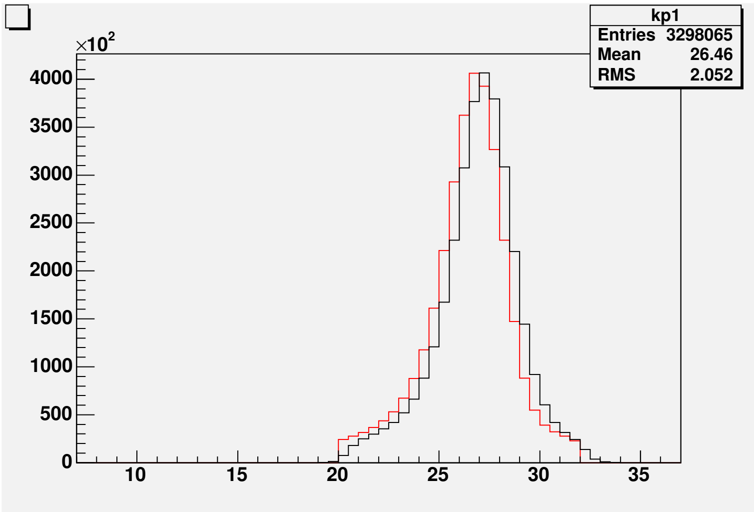


Fig. 9: *Kinematic peak.*

## Acknowledgments

First I want to thank my supervisor Dr Ewelina Lobodzinska for her patience and invaluable help. Secondly I want to thank the organisers of the DESY Summer Student Programme 2004.

## References

[1] http://www-h1.desy.de

[2] A.A. Glazow, Measurement of the Proton Structure Functions $F_2(x, Q^2)$ and $F_L(x, Q^2)$ with the H1 Detector at HERA, Berlin 13.02.1998

[3] T. Lastovicka, Measurement of the Inclusive Deep inleastic Scattering Cross Section at low $Q^2$, Berlin 7.05.2004

[4] ROOT Users Guide 3.10, Dec, 2003